

# PREDICTING MUD MOTOR PERFORMANCE AND RELIABILITY WITH REDUCED ORDER MODELING

ANTON KOLYSHKIN<sup>1</sup>

<sup>1</sup>Schlumberger Technology Corp.  
23400 Colonial Pkw., Katy, TX 77493, USA  
AKolyshkin@slb.com and www.slb.com

**Key words:** FEM, Mud Motors, Elastomer Modeling

**Abstract.** In this paper we present a reduced order model for simulating mud motor performance and reliability. The model breaks down a mud motor power section to a set of 2D simulations with simplified drilling fluid flow description. It can reliably predict power curves and failure risks caused by elastomer fatigue, hysteresis heating, and debonding. The model can capture mud compatibility effects as well. Due to relatively short simulation time, it becomes feasible to perform simulations for new motor design, elastomer, failure analysis, or to find optimal motor type, elastomer, interference fit, and differential pressure for a specific job.

## 1 INTRODUCTION

Mud motors have been widely used in directional drilling since the 1960s. They are rather cheap and commoditized, robust and powerful, and easy to manufacture and maintain. It is believed that more than 60% of directional drilling jobs are performed with mud motors. Even after introduction of advanced rotor steerable systems (RSS) in the 2000s, the usage of mud motors did not decrease, as apparently coupling a mud motor and RSS brings synergetic effects of improved control and drilling speed, so now some motors are specifically designed for such application.



**Figure 1.** Mud motor layout

A mud motor consists of three main parts: power section, transmission, and bearing section (Figure 1). The power section is responsible for torque generation, i.e. it converts hydraulic energy of drilling fluid to mechanical energy of planetary rotor rotation. The transmission transforms planetary rotation to simple rotation and possibly passes it through some angle formed by the motor corpus. The bearing section takes the axial load from rotor and transmission. The mud motor drives the drilling bit either directly or through RSS.

Power section assemblies are the most critical part of the mud motors [1]. Mud motor

performance and reliability mostly depend on power section design and materials. The power section is the most sensitive to operating conditions and generally defines the motor operating conditions. Most mud motor failures are, in fact, power section related.

The power section itself consists of two parts: rotor and stator (Figure 2). The mud motor rotor is usually made of stainless steel and coated either with hard chrome or tungsten carbide to give extra protection from corrosion and abrasion. The mud motor stator is typically a metal tube (optionally profiled), which has rubber lining inside. Both rotor surface and stator interior have special helical surfaces, so, when assembled, they form a set of closed cavities. The rotor can perform planetary motion inside stator. During such rotation, the cavities move along the power section while remaining sealed.

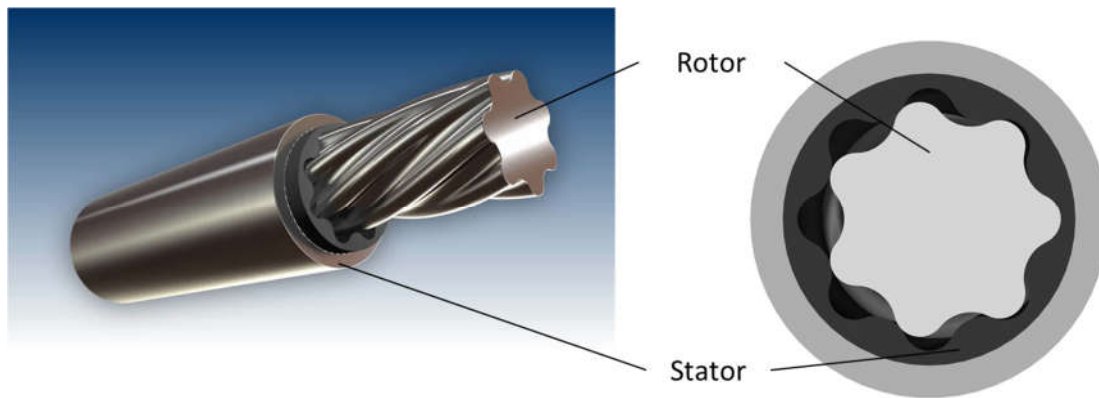


**Figure 2.** Power section layout

So, if the cavities are filled with a fluid and the rotor is forced to rotate, the whole mechanism will work as a pump [2]. Vice versa, if the fluid is pumped through the power section under pressure, it will make the rotor rotate. That's the way a mud motor works.

The power sections are categorized by number of lobes (the rotor has always one less lobe than a stator), their profile, size or outer diameter, length, number of stages, elastomers, and interference fit between the rotor and stator. All these parameters affect the mud motor performance and reliability.

Mud motor performance is usually represented in a form of power curve (Figure 3), which links together pressure across the motor, torque, and rotation speed. At low differential pressure, the rotor rotation speed is quite constant, and the torque response is almost linear. However, when the pressure is growing, the stator elastomer is subjected to a higher deformation level. At some point, stator elastomer lobes are deflected enough to break up sealing between cavities. Thus, a portion of the drilling fluid starts leaking through the motor without producing useful work and the rotation speed consequently declines. Also, the increasing elastomer deformation and distorted geometry result in mechanical losses, which reduce the slope of the torque curve at high pressure.

It is quite important to select a motor with adequate performance. Depending on the drilling job parameters, bit type, and formation, there are certain torque and rpm requirements. If the motor cannot provide them, it may result in low drilling speed (ROP), frequent stalls, excessive vibrations and wear, and poor directional control.

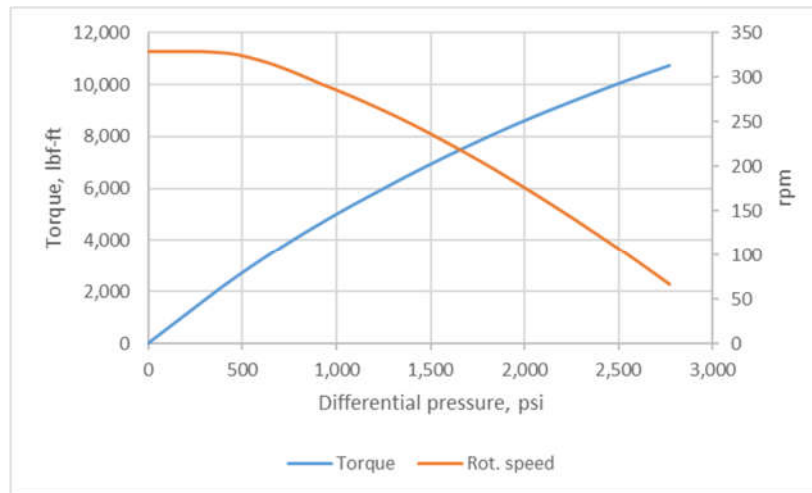


Figure 3. Power curve example

Mud motor performance can be measured under controlled conditions on surface, however, it is a nontrivial task to extrapolate these results to downhole conditions, where it differs by elevated temperatures, pressure, and drilling fluids. So, modeling the downhole performance may be the only available choice in the case of mud motors.

From the reliability aspect, it is anticipated that motors can be run under certain conditions for the entire job duration without failure, including either complete loss of functionality or substantial loss of performance. In such scenarios, in many cases, the drilling job cannot be continued, and the motor is replaced. However, to replace a motor, one needs to pull out the entire drillstring, which is quite costly and time consuming.

The most common root causes of mud motor failures are hysteresis or fatigue chunking, debonding, and abrasion wear of stator elastomer. So, mud motor modeling is anticipated to provide failure risk estimation under downhole conditions predicting type and probability of the failure and possibly motor lifespan.

## 2 MODELING CHALLENGES AND OBJECTIVES

Despite being quite simple in design, the power section of a mud motor is very challenging for modeling. The first problem is quite complex kinematics. The rotor performs planetary rotation inside the stator, which is identical to a circle rolling inside a bigger circle (Figure 4). Thus, the rotor not only rotates in the external reference frame, but its center rotates around the stator center as well. The contact between rotor and stator lobes changes from pure sliding to pure rolling.

Then, the stator elastomer brings to the model nonlinear friction, large deformations, and viscoelasticity. This requires more characterization, increases model complexity, and boosts the computation cost.

Finally, interaction with the drilling fluid must be taken into account as well. The drilling fluid hydrodynamics is a key for mud motor performance modeling. In addition, the drilling fluid can interact chemically with the elastomer, changing its properties.

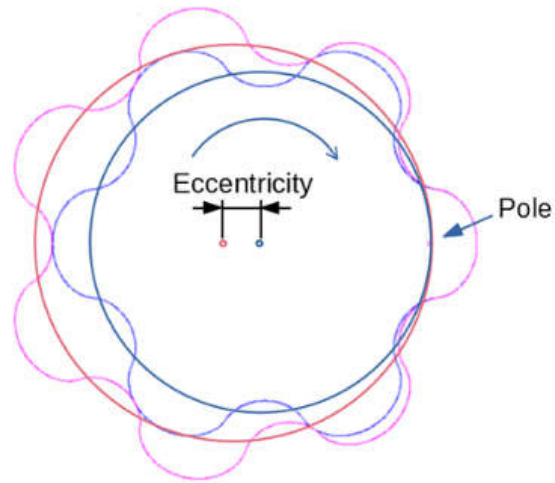


**Figure 4.** Rotor motion is similar to a circle roiling in another circle

There have been several published works dedicated to mud motor modeling, however, many of them had to sacrifice one or more aspects mentioned above. In some publications the authors used fully theoretical approach [3], empirical [4] or based on big data [5]. There are several papers showing results of modeling a particular aspect of mud motor operations, like fluid dynamics [6], hysteresis [7] or kinematics [8].

Some time ago, we developed a full-scale 3D FSI model, which couples FEA and CFD to derive motor performance and reliability [9]. It managed to properly predict many effects, like elastomer deformation, pressure distribution, drilling leakages, and rotor bending. However, it took a significant amount of computation time, limiting its engineering usage, and it lacked some important effects as well, for example, hysteresis heating.

Because downhole operating conditions vary significantly, the power section portfolio has hundreds of models, and there is always a choice of a different elastomer or interference fit, we need to have a modeling tool which can predict motor performance and reliability in a reasonable amount of time. So, while working on the full-scale 3D model, we have been developing a reduced order model with simplified geometry and some physical processes. The primary focus was reduction of computation costs to make the model an effective engineering tool.

### 3 THE MODEL DESCRIPTION

In order to have a fast and scalable algorithm, two major simplifications have been made in the model:

- a set of 2D simulations is conjugated to represent dynamic behavior of stator elastomer;
- drilling fluid dynamics are reduced to a cavity network, which is connected through gaps, and there is no mechanical interaction between the fluid and elastomer.

The first assumption is based on the periodicity of power section geometry and the fact that due to the rotor motion inside stator, each stator cross section is dynamically equal to another. If rotor and stator are undeformed and the eccentricity is constant over the entire length of the power section, each subpitch becomes identical to any other (Figure 5a). So, assuming small

rotor and stator deformation, when modeling a power section, we can reduce the full power section geometry to just one pitch length.

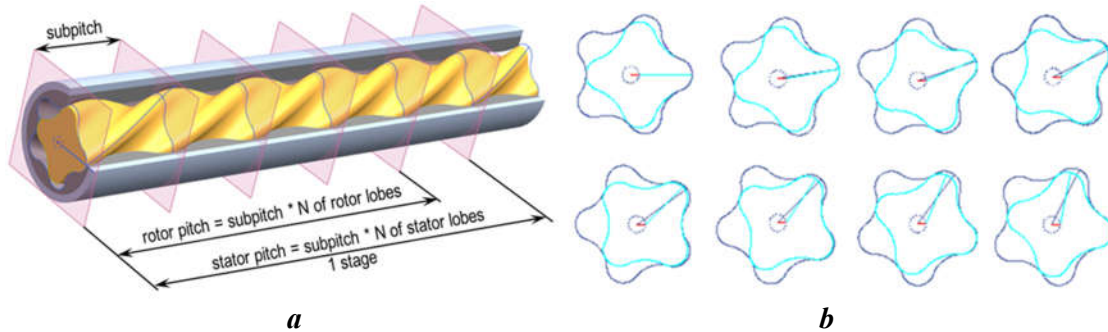


**Figure 5:** Power section geometry periodicity (a) and relative rotor position in different cross sections (b)

In addition, within subpitch, each 2D cross section is identical as well. While the moving rotor is taking all possible positions inside the stator (Figure 5b), all cross sections undergo the same deformation cycle, but shifted in time. The shift in time is proportional to the distance between them and the rotation frequency.

Furthermore, the stators and rotors of mud motor power sections are normally designed to have identical lobes. So, each lobe of multilobe stator undergoes exactly the same deformation cycle as any other as well. We can effectively use this feature to increase the time resolution of the deformation cycle.

Thus, the model treats the power section as if the geometry, the displacements, the deformation, and the forces follow the same cycle for every lobe in all cross sections. Assuming that the deformation in the direction of the power section axis is substantially smaller than in the perpendicular directions, which is confirmed by 3D modeling, we can perform 2D modeling for several orientations of the rotor and stator, then derive full deformation cycle and use it to reconstruct 3D geometry. This approach is anticipated to be very relevant in the middle of the power section, however, it may result in some potentially higher deviations at both ends.

The FEA mesh is created only for stator elastomer, assuming the stator tube and rotor to be infinitely rigid. Nonlinear elasticity model is used as constitutive model of rubber [10]. This model requires only simple tension test results and bulk modulus. Since rubber elasticity significantly depends on temperature, the normal practice is to perform the tests in the temperature range from ambient to up to 200 degC, which completely covers mud motor field applications.

The FEA is performed for different relative orientation between the rotor and the stator. All the orientations are linked through the rotor orbit constrains. The solutions can be decomposed into time sequences of rotor motion and elastomer deformations. This time sequence is looped, i.e., it represents full deformation cycle and is used for hysteresis processing.

In simple words, hysteresis is a lapse between deformation and stress response in cyclic loading. The phase angle between them, or namely its tangent value  $\tan \delta$  is used to characterize elastomer viscoelasticity. It normally depends on loading frequency, amplitude, and temperature, thus, a set of tests under different conditions is required for proper characterization.

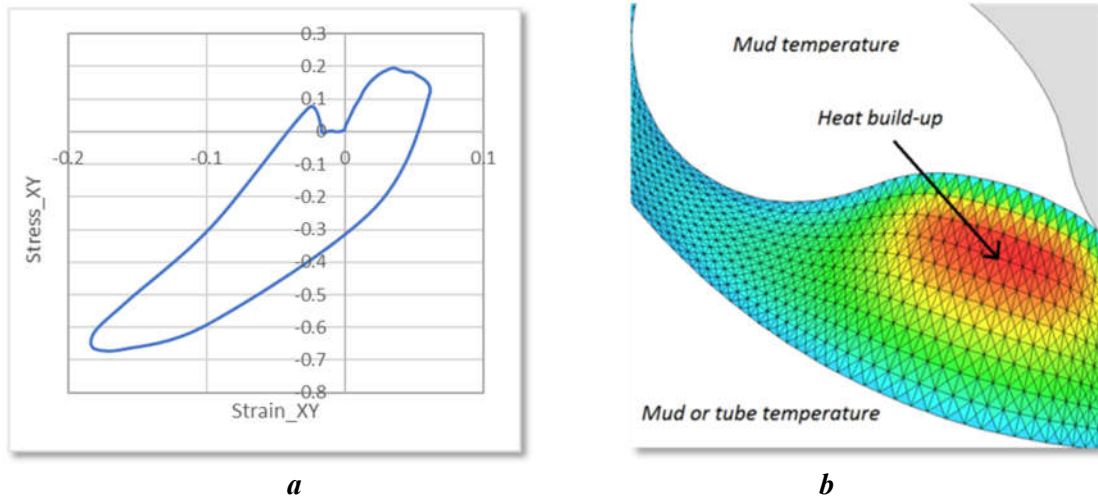


**Figure 6.** Hysteresis loop (a) and temperature field (b) of a power section.

In order to apply viscoelasticity, fast Fourier transform (FFT) is performed for each element of the model. It results in modified element stress, which is used as input for next iteration of the FEA. After several iterations FEA>FFT>FEA, the stress and strain values converge with some reasonable tolerance, and we have hysteresis loop for each element in the strain-stress coordinates. (Figure 6a). The area within the loop effectively is the deformation energy loss due to the heat per deformation cycle. The heat buildup rate is the product of the loading frequency and heat loss per cycle. By having heat buildup rate for each element and mud temperature as boundary conditions (Figure 6b), we can solve either steady or transient thermal problems and get temperatures in each element. This temperature field can be used to adjust material properties and get more accurate simulation results on the next iteration, but also high internal temperature itself indicates the risk of hysteresis chunking. The deformation cycle is also used to predict fatigue life in each element in stator elastomer under certain conditions by utilizing either Lake-Lindley or Tomas model [11].

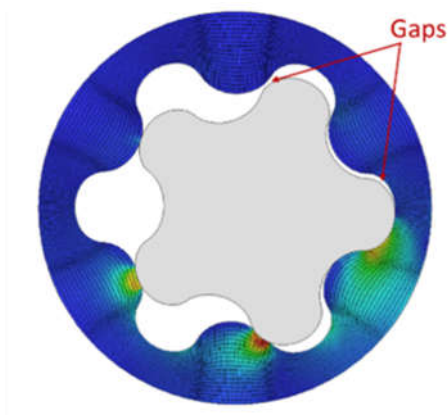


**Figure 7:** Gaps between rotor and stator.

To determine the loading frequency, and hence, hysteresis heat buildup and fatigue life in hours, one needs to know the motor rpm. Theoretically the motor rpm is proportional to the flow rate, however, due to the rubber deformation, some gaps appear between adjacent cavities (Figure 7) forming path to drilling fluid leakages and, thus, loss of rpm. The rpm reduction is proportional to the fluid loss through leakages.

In order to find the amount of leakages, we determine the gap area between cavities and use the orifice plate model for incompressible fluid. The pressure in the cavities and torque are determined from the rotor force balance.

The entire algorithm is implemented as standalone executable code, which is available to power section designers and engineers and can be embedded into higher level systems [12].

#### 4 MODELING RESULTS

The model takes as input real stator and rotor profiles, power section length, and pitch. The required elastomer properties include stress-strain curves,  $\tan \delta$  values at different temperatures, coefficients for fatigue models, friction parameters for Thirion equation [13], optionally parameters for Mullins softening, permanent set, and abrasion. The operating conditions include flow rate, downhole temperature, and pressure. There is also an option to include mud diffusion into elastomer, which may cause volume change and affect rubber stiffness and fatigue life.

The algorithm enables predicting power curves depending on operating conditions. The model predictions match physical measurements quite well (Figure 8) and can be done for downhole conditions (Figure 9). Better knowledge of downhole performance gives better control of drilling process and higher ROP. If modeling is performed at the job planning stage, it enables proper motor configuration and interference fit selection. The interference fit is quite an important factor, as low fit may result in insufficient performance, but excessive fit may impact motor reliability.

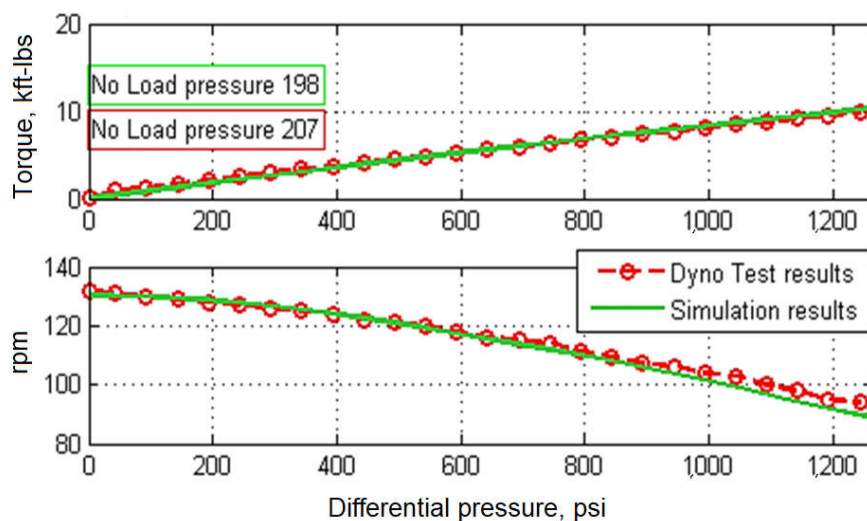
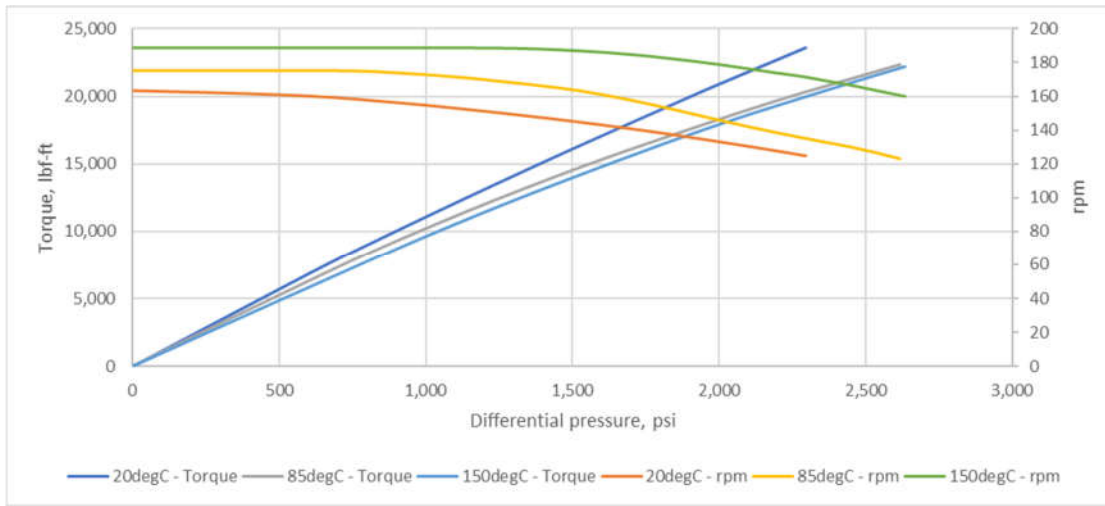


Figure 8. Power curves simulation vs. Dyno test at ambient temperature.



**Figure 9.** Power curves evolution with temperature

The mud motor reliability can be considered through three main risks: fatigue, hysteresis, and debonding. Fatigue is the process of gradual initiation of microscopic cracks and their subsequent growth to macroscopic size under cyclic load. During typical mud motor lifespan, the elastomer is subjected to some millions of deformation cycles, so fatigue failure is a rather common issue.

The debonding process is similar to the fatigue, however, in the case of debonding, the cracks appear and propagate at the interface between rubber and metal. Both fatigue and debonding finally result in the disintegration of elastomer lining and loss of motor ability to deliver power.

The crack growth rate depends on cracking energy density (CED) in case of fatigue and debonding energy (DE) in case of debonding, both being a portion of strain energy available for crack growth in a given direction [14]. Typically, the higher the CED and DE values, the more failure risk it imposes. In case of fatigue, we can perform elastomer characterization for the fatigue models, which can predict service life of motor in hours.

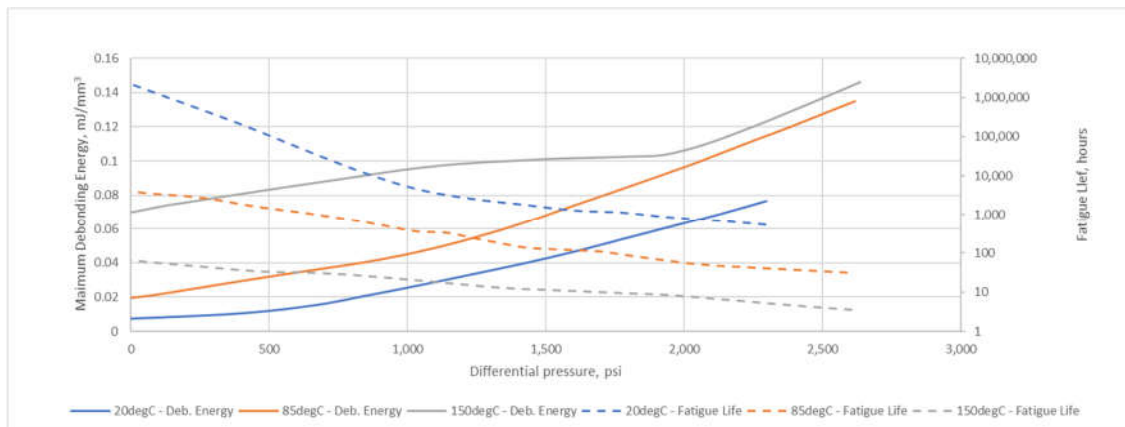


**Figure 10.** Fatigue life and debonding energy at different temperatures

Figure 10 shows how the fatigue life and debonding energy depend on differential pressure and temperature for the same power section. Growing differential pressure reduces fatigue life because of higher deformation level. The temperature has two effects in increasing interference fit and weakening the elastomer. As the result, if there is negligible risk of fatigue failure at 20 degC, at 150 degC the predicted fatigue life is lower than 100 h, even at small differential pressures. Although it is not possible to avoid elastomer weakening at high temperatures, adjusting the interference fit could improve the situation.

Hysteresis heating can promote fatigue or debonding or may cause failure by itself. During cyclic deformation, some part of deformation energy is lost and released as heat during each cycle. Mud motor typical loading frequencies lay in the range of 10–30 Hz, so it can be a tremendous amount of heat. Rubber is a poor heat conductor, thus, the temperature inside the rubber lobe may significantly exceed mud temperature or even reach the value sufficient to start rapid chemical degradation. As the growing temperature causes rubber thermal expansion and hence, the growth of the interference fit, the deformation energy grows as well, and in some circumstances may form positive feedback.

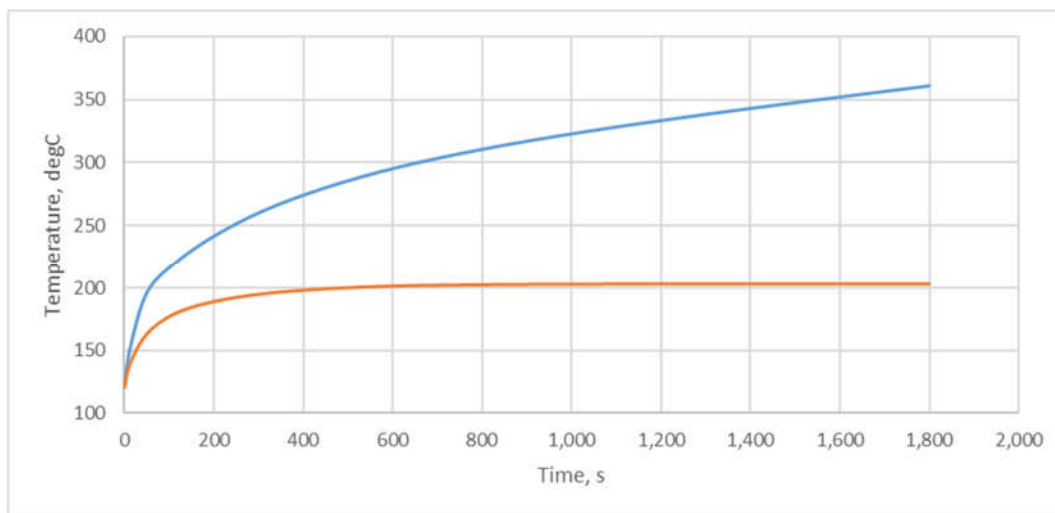


**Figure 11.** Maximum temperature evolution for two elastomers

Figure 11 gives an example of such feedback. It shows how the maximum elastomer temperature will evolve in two power sections run under constant load. The power sections differ only by elastomer type, which have different value of  $\tan \delta$ . The elastomer with the lower value approaches equilibrium after about 10 minutes. In the case of the other elastomer, the amount of generated heat is higher, and the continuing thermal expansion does not reach the equilibrium. In practice it means that the elastomer temperature reaches a dangerous level with its rapid deterioration and consequent failure.

The chemical interaction between drilling fluid and stator elastomer can also alter power section performance and reliability. The drilling fluid can diffuse in the elastomer or extract its components causing its volume and stiffness and fatigue life reduction as well. To take the effects into account, we can model mud diffusion in the elastomer (Figure 12) and modify each element property to include mud effect.

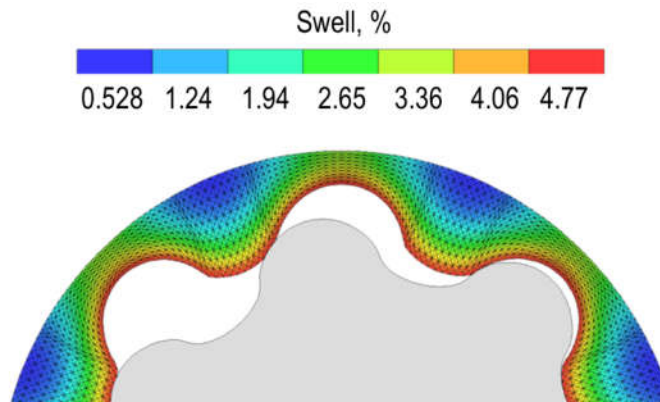


**Figure 12.** Stator elastomer swell distribution

This way we can simulate performance and reliability after some prolonged contact with a drilling fluid, like shown on Figure 13. As seen there, 100 h contact with oil-based mud caused a significant swell of elastomer in conjunction with weakening, decreasing the estimated fatigue life by few orders of magnitude. In this case, the reduction of the failure risk can be achieved by adjusting the interference fit and optionally replacing the elastomer for more resistant one to this type of the drilling fluids.

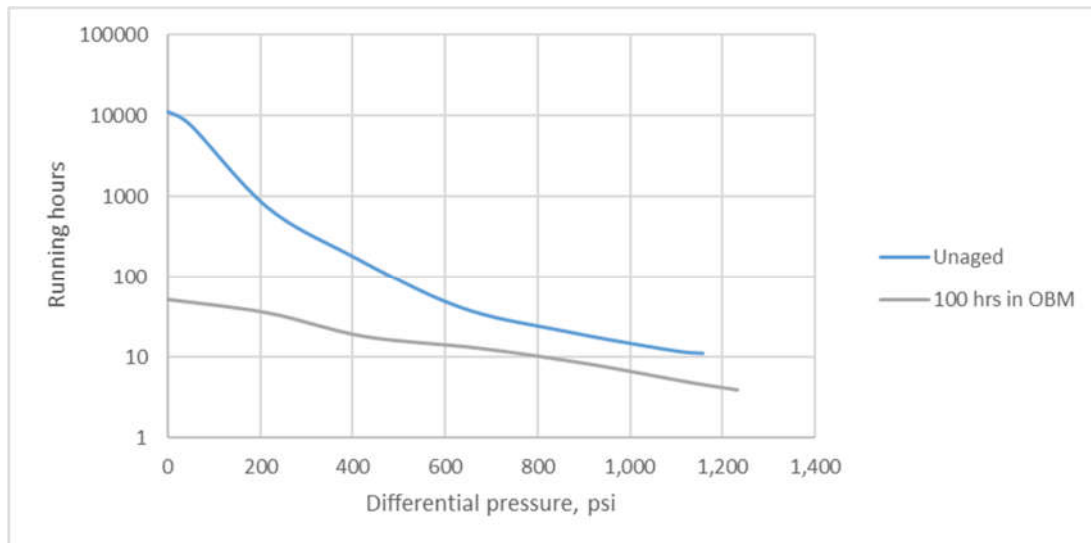


**Figure 14.** Mud compatibility effect on power section fatigue life.

All the simulations discussed above can be performed in a rather small amount of time. For example, simulation at one particular load condition, e.g. constant torque or pressure, takes several minutes, deriving a power curve takes less than an hour, and hysteresis simulation for constant load can be done within 20 minutes. That enables using this model for routine engineering tasks, as power section design optimization, motor selection during job planning,

and failure analysis.

It drastically improved motor reliability and solved long-lasting problems with drilling efficiency, as shown in [15]. It was used in development of new commercially available elastomers with higher pressure rating. The model predictions are used to perform a cumulative damage analysis to assess the risk of extending the usage of a motor [16]. Finally, abundance of modeling results enabled some higher level systems designed for motor usage optimization.

## 5 CONCLUSIONS

We developed a reduced order model of mud motor power section, which enables predicting mud motor performance and reliability depending on:

Real stator and rotor geometry, elastomer properties, interference fit, downhole temperature, flow rate, mud compatibility

The results are output as physical quantities and may include:

pressure, torque, rpm, fatigue life in cycle or hours, bonding stress or debonding energy, maximum temperature due to hysteresis heating

Thus, from a technical point of view, the reduced order model enables:

- selecting an optimal power section, elastomer, and interference fit for given conditions, which provides both adequate performance and reliability;
- perform failure analysis;
- optimize power section design;
- provide recommendations for optimal operating conditions;
- derive elastomer properties to meet performance and reliability requirements.

## REFERENCES

- [1] Tiraposlky, W. *Hydraulic Downhole Drilling Motors: Turbodrills and Positive Displacement Rotary Motors*. Houston: Houston Gulf Publishing Co. (1985).
- [2] Moineau, R. J. L. Gear Mechanism. *Patent US-Patent 1 892 217*. (1931).
- [3] Nguyen, Tan C., E. Al-Safran, and V. Nguyen. "Theoretical modeling of positive displacement motors performance." *Journal of Petroleum Science and Engineering* 166 (2018): 188-197.
- [4] Yáñez, E., Arredondo H., Micksu H. "Management and Best Practices of Progressive Cavity Pumps Failures Huyaparí Field, Orinoco Oil Belt." *Paper presented at the SPE Artificial Lift Conference-Americas, Cartagena, Colombia, May 2013*. doi: <https://doi.org/10.2118/165061-MS>
- [5] Zhang, Zh., Shen, Y., Chen, W., Zhenyu Ch.. "Analyzing Energy and Efficiency of Drilling System with Mud Motor through Big Data." *Paper presented at the SPE Annual Technical Conference and Exhibition, Virtual, October 2020*. doi: <https://doi.org/10.2118/201502-MS>
- [6] Paladino, E., Alves de Lima, J, Almeida, R., Assmann B.W. "Computational Modeling of the Three-Dimensional Flow in a Metallic Stator Progressing Cavity Pump." *Paper presented at the SPE Progressing Cavity Pumps Conference, Houston, Texas, USA, April 2008*. doi: <https://doi.org/10.2118/114110-MS>
- [7] Delpassand, M. S.). "Stator Life of a Positive Displacement Downhole Drilling Motor."

- ASME. J. Energy Resour. Technol. June 1999*; 121(2): 110–116.
- [8] Aage, N., Donaldson, J., and Feng, Y. "Mathematical Problems for Moineau Pumps." *57th European Study Group Mathematics with Industry (ESG157)*. (2006). 1–48
- [9] BA, S., Pushkarev, M., Kolyshkin, A., Song, L., Yin L.L.. "Positive Displacement Motor Modeling: Skyrocketing the Way We Design, Select, and Operate Mud Motors." *Paper presented at the Abu Dhabi International Petroleum Exhibition & Conference, Abu Dhabi, UAE, November 2016*. doi: <https://doi.org/10.2118/183298-MS>
- [10] Kasper, William J. Constitutive models for engineering materials. *Encyclopedia of Physical Science and Technology. Third Edition*. V.3 (2002). 603-633
- [11] Lindley PB. Energy for crack growth in model rubber components. *Journal of Strain Analysis*. 1972;7(2):132-140. doi:10.1243/03093247V072132
- [12] BA, S., Belov, D., Nobre, D., Yin, L. L., Johnson, E.. "Combined Data Analytics and Physics-Based Simulation for Optimum Bit, Motor, BHA Combination." *Paper presented at the Offshore Technology Conference Brasil, Rio de Janeiro, Brazil, October 2019*. doi: <https://doi.org/10.4043/29875-MS>
- [13] Thirion, P. *Rev. Gen. Caoutch.*, 23, 101 (1946).
- [14] Mars, W. V. Cracking Energy Density as a Predictor of Fatigue Life under Multiaxial Conditions. *Rubber Chemistry and Technology 1 March 2002*; 75 (1): 1–17. doi: <https://doi.org/10.5254/1.3547670>
- [15] Beeh, H. A., Nobre, D., Ba, S., Yan, X. , Lauritsen, Å. , Døssland, Ø. , Hodne, J. "Drilling a Challenging Kvitebjørn Field 5<sup>3/4</sup>-in. Section in a Single Run Using a New Mud Motor Modeling Engineering Workflow and New Long-Life Elastomer." *Paper presented at the SPE Norway One Day Seminar, Bergen, Norway, April 2018*. doi: <https://doi.org/10.2118/191331-MS>
- [16] S. Ba, A. Kolyshkin. Determining the life span of an elastomer in a motor. *Patent US-Patent 10139326* (2018).